ORIGINAL ARTICLE

Whole-exome sequencing identified two novel mutations of *DYNC2LI1* in fetal skeletal ciliopathy

Xinyue Zhang[1] [iD] | Yanqin You[1] | Xiaoxiao Xie[1] | Hong Xu[2] | Honghui Zhou[1] | Yuanmei Lei[3] | Pei Sun[4] | Yuanguang Meng[1] | Longxia Wang[2] | Yanping Lu[1]

[1]Department of Obstetrics and Gynecology, 1st Medical Center of Chinese, PLA General Hospital, Beijing, China

[2]Department of Ultrasound, 1st Medical Center of Chinese, PLA General Hospital, Beijing, China

[3]Department of Dermatology, 1st Medical Center of Chinese, PLA General Hospital, Beijing, China

[4]Beijing Genomics institution, Beijing, China

Correspondence
Longxia Wang, Department of Ultrasound, 1st Medical Center of Chinese PLA General Hospital, Beijing, China.
Email: 13693685342@163.com

Yanping Lu, Department of Obstetrics and Gynecology, 1st Medical Center of Chinese PLA General Hospital, Beijing, China.
Email: luyp301@163.com

Funding information
This work was supported by the funds from the Translational Medical Foundation of Chinese PLA General Hospital (no. 2018TM-11).

Abstract

Background: Skeletal ciliopathies are a group of clinically and genetically heterogeneous disorders with the spectrum of severity spanning from relatively mild to prenatally lethal. The aim of our study was to identify pathogenic mutations in a Chinese family with two siblings presenting a Short-rib polydactyly syndrome (SRPS)-like phenotype.

Method: Karyotyping and NGS-based CNVseq were performed. Obtaining the negative results in karyotyping and CNVseq, whole-exome sequencing (WES) using genomic DNA (gDNA) extracted from the umbilical cord blood of the first fetus was carried out, followed by bioinformation analysis. The candidate pathogenic variants were confirmed by Sanger sequencing in the family.

Results: No chromosomal abnormalities and pathogenic copy number variations (CNVs) were detected in the affected fetus with SRPS-like phenotype. WES analysis identified two novel compound heterozygous variants in *DYNC2LI1*, c.358G>T (p.Pro120Ser; NM_001193464), and c.928A>T (p.Lys310Ter; NM_ 001193464). Bioinformatics analysis suggested that c.358G>T (p.Pro120Ser) was likely pathogenic and c.928A>T (p.Lys310Ter) was pathogenic. Sanger sequencing of the two variants in family reveal that c.358G>T was from paternal origin and c.928A>T was from maternal origin, and the second affected fetus had the same compound heterozygous variants in *DYNC2LI1*. Definitive diagnosis of short-rib thoracic dysplasia 15 with polydactyly (SRTD15) was made in the family.

Conclusion: Our results expand the mutational spectrum of *DYNC2LI1* in severe skeletal ciliopathies. WES facilitates the accurate prenatal diagnosis of fetal skeletal ciliopathy, and provides helpful information for genetic counseling.

KEYWORDS

DYNC2LI1, short-rib thoracic dysplasia 15 with polydactyly (SRTD15), skeletal ciliopathy, whole-exome sequencing

1 | INTRODUCTION

Skeletal ciliopathies are a rare group of genetic disorders that result from deficits of primary cilium. They are characterized by skeletal anomalies such as short limbs and ribs, and brachydactyly or polydactyly. Skeletal ciliopathies include short rib-polydactyly syndromes (SRPSs), asphyxiating thoracic dystrophy (ATD, or Jeune syndrome), Ellis-van Creveld syndrome (EVC), Mainzer-Saldino syndrome (MZSDS), and cranioectodermal dysplasia (CED, or Sensenbrenner syndrome), most of which are autosomal recessive disorders (Baker & Beales, 2009; Mortier et al., 2019; Waters & Beales, 2011). Because of clinically and genetically heterogeneous conditions with overlapping phenotypic features, the diagnostic diagnoses between these diseases are challenging (Braun & Hildebrandt, 2017; Mitchison & Valente, 2017).

SRPSs characterized by short ribs and narrow thorax, polydactyly, short limbs, and multiorgan anomalies are prenatally lethal due to extremely narrow thorax of the affected fetuses (Huber & Cormier-Daire, 2012). Formerly, SRPS was classified into four subtypes based on clinical phenotype and radiological features (Elcioglu & Hall, 2002). Though abnormal fetuses with SRPS could be detected by prenatal ultrasound due to observably short femurs and narrow thorax, it is almost impossible for clinician and geneticist to make a differential diagnosis.

The identification of mutations in genes encoding proteins in cilium has facilitated the confirming the specific SRPS subtypes (Badiner et al., 2017). Advances in next generation sequencing (NGS) technology and bioinformatics analysis have significantly boosted the discovery of underling genetic causes of genetic bone diseases (Mortier et al., 2019; Zhang et al., 2018). Molecular analysis of potential causative genes has become a feasible and acceptable approach to provide genetic counseling and predict recurrence risk. Nowadays, targeted next generation sequencing and Whole-exome sequencing (WES) are undoubtedly powerful approaches of detecting underlying causative genetic variants in clinical practice (Chandler et al., 2018; Liu et al., 2019; Petrovski et al., 2019). Here, we performed WES in a Chinese family with two consecutive pregnancies SRPS-like fetuses and the etiologic diagnosis was finally made.

2 | MATERIALS AND METHODS

2.1 | Ethical compliance

The present study was approved by the ethics committee of Chinese PLA General Hospital (approval no. S2019-112-01). Written informed consents were obtained from the pregnant couple.

2.2 | Clinical information

The pregnant woman was referred to the prenatal diagnosis center of the first center of Chinese PLA General Hospital twice due to fetal multiple anomalies. The pregnant couple were physically healthy and non-consanguineous. No family history of genetic diseases was found in their families. She previously underwent two spontaneous abortions in the 7 weeks of pregnancy with no obvious pathogenesis.

Abnormal ultrasound findings of both affected fetuses were further confirmed by the sonographers qualified for prenatal diagnosis. Due to the severe and probably lethal anomalies, the pregnancies were terminated under the couple' request at 26th week of gestation age (GA) and 22nd GA, respectively. Tests of the abortuses, including radiographic examination, autopsy, karyotyping, NGS-based CNVseq, and whole exome-sequencing (WES) were performed.

2.3 | Prenatal ultrasound examination

Prenatal ultrasound was undertaken to scan abnormal fetuses. Fetal biometric data were examined and compared with normal values, including measurements of biparietal diameter (BPD), length of femur and humerus (FL and HL), head circumference (HC), abdominal circumference (AC), amniotic fluid volume (AFV), thoracic morph, and additional malformations. After abnormal ultrasound findings were monitored, a senior sonographer was used to confirm the ultrasound report.

2.4 | Karyotyping and NGS-based CNVseq

Fetal umbilical cord blood samples were obtained for chromosome G band karyotype analysis according to standard operating procedures. Chromosomal description and naming were based on the International System for Human Cytogenetic Nomenclature (Simons et al., 2013).

Genomic DNA (gDNA) was extracted according to the instructions of genomic DNA extraction kit (Qiagen Inc., Hilden, Germany) from the fetal umbilical cord blood. Library preparation was in accordance with standard operating procedures. High-throughput sequencing was performed on Illumina NovaSeq 6000 series sequencer (Illumina Inc., San Diego, USA). Reads were mapped to reference genome hg19 using the BWA software. Chromosomal DNA affected at >100 kb was identified as a copy number variation (CNV). CNVs were classified according to American College of Medical Genetics (AGMG) guidelines (Kearney et al., 2011).

2.5 | Whole-exome sequencing (WES) and bioinformatics analysis

Genomic DNA was isolated from Fetal umbilical cord blood were sheared by sonication (Covaris S-seriesTM, USA). The sheared genomic DNA was used for construction of the indexed libraries according to manufacturer's protocol (NGS Fast DNA Library Prep Set for Illumina, Joy Orient, China). The genomic library was then hybridized with xGen® Exome Research Panel v1.0 probe sequence capture array of IDT (Integrated Device Technology®, USA), to enrich the exonic region (Joy Orient, China). The libraries were first tested for enrichment by qPCR and for size distribution and concentration using the Agilent Bioanalyzer 2100. Exon-enriched DNA was sequenced by the Illumina Hiseq™ XTen platform following the manufacturer's instructions (Illumina®, USA).

Raw image files were processed by the BclToFastq (Illumina®, USA) for base calling and generating the raw data. The sequencing reads were aligned to the NCBI human reference genome (hg19) using BWA. Samtools and Pindel were used to call single nucleotide polymorphisms (SNPs) and insertions or deletions (InDels) of the sequence. Variants in intronic region (beyond 30 bp from exon-intron boundary), SNVs with low-quality (Allele Frequency <0.2, sequencing depth <4x, or mapping qualities <35), InDels in simple sequence repeat region (SSR >7 and Allele Frequency <0.3), and long InDels (length >50 bp) and were preliminarily filtered. Variants were annotated by ANNOVAR. All single nucleotide variants (SNVs) and InDels were annotated with public population frequency databases, including NCBI dbSNP, 1000 Genomes Project, the Exome Aggregation Consortium (ExAC), as well as OMIM, Swiss-var, Human Gene Mutation Database (HGMD), ClinVar, and other disease databases. The variants that were not in any database were considered novel. All synonymous substitutions or SNPs with MAF (Minor Allele Frequency) higher than 5% were filtered out. Seven well-established silico prediction programs, including Scale-Invariant Feature Transform (SIFT), PROVEAN, LRT, PolyPhen-2, MutationTaster, and CADD were used to functional predict of the effect of missense variants. Pathogenicity of variants were assessed under the protocol issued by ACMG (Tavtigian et al., 2018). The identified candidate causative variants related to skeletal ciliopathy were finally confirmed in the family by Sanger Sequencing.

3 | RESULTS

3.1 | Fetal abnormal presentation

Both of the pregnancies were terminated by induction of labor in the second trimester. Clinical and genetic findings are presented as follows:

3.2 | Fetus 1

A routine ultrasound at 23 weeks of gestation showed multiple anomalies of the fetus, including short limbs (femur length 2.43 cm; humeral length 2.39 cm), a narrow thorax, mild kyphosis of lumbar vertebra, multiple cardiac abnormalities, acromphalus, and transposition of abdominal organs (Figure 1). Autopsy of the fetus was performed, and additional malformations, postaxial polydactyly of hands
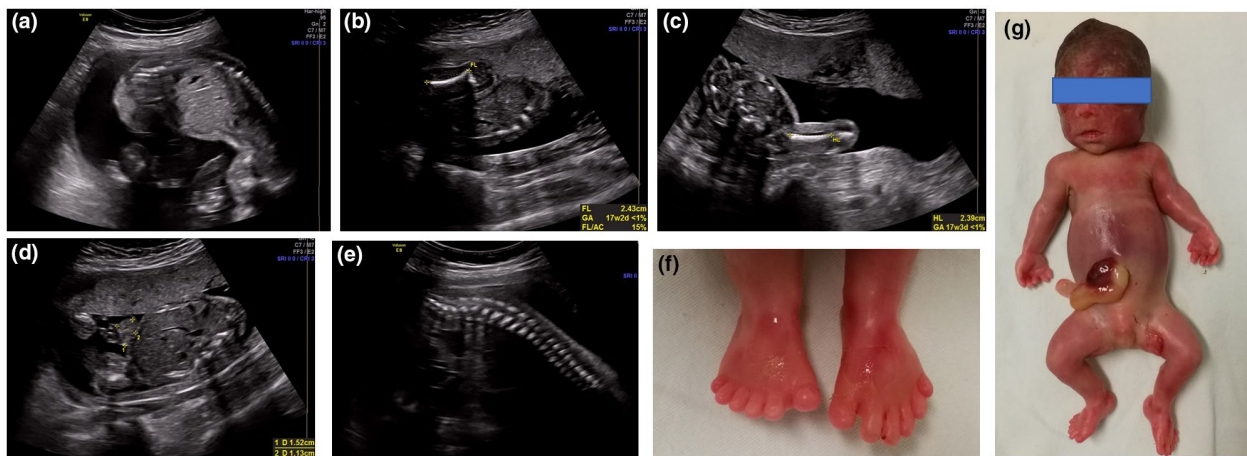

FIGURE 1 (a–e) Prenatal ultrasound of Fetus 1 at 23 weeks of gestation. A narrow thorax and a relatively enlarged abdomen (a), shortened limbs (FL 2.43 cm and HL 2.39 cm, <1th percentile of the GA) (b and c), multiple cardiac abnormalities, including single ventricle and ventricular septal defect (d), acromphalus (e). (f and g) Appearance of the aborted fetus. postaxial polydactyly of feet (f) and appearance of the whole body (g). AC, abdominal circumference; FL, femur length; GA, gestational age; HL, humerus length

and feet, were found (Figure 1). Radiographic examination was absent.

3.3 | Fetus 2

Multiple anomalies, including a narrow thorax, lumbar kyphosis, short and curved limbs (femur length 2.41 cm; humeral length 2.05 cm), and polydactyly (Figure 2) were detected by ultrasound at 21 weeks of gestation. Termination of the pregnancy was performed at 22 weeks gestation after informed consent from the couple. X-ray scan was performed, and showed that the fetus presented a markedly narrow thorax and short ribs (Figure 2). No other abnormal features were detected by autopsy.

3.4 | Karyotyping and CNVs

Chromosomal abnormalities and submicroscopic chromosomal imbalances were not be detected in Fetus 1.

3.5 | WES and bioinformatics analysis

The WES strategy of Fetus 1 reached an average sequencing depth of 95.93X. The average coverage of the whole exons for >20 reads were 98.88%. A total of 60,129 variants were identified, including 53,574 SNVs and 6,555 InDels. Filtering following the above-mentioned analysis strategy, two compound heterozygous variants in *DYNC2LI1*, c.358G>T (p.Pro120Ser; NM_ 001193464), and c.928A>T (p.Lys310Ter,43; NM_ 001193464), were identified as causative mutations for the affected Fetus 1 (Table 1). Bioinformatics analysis of *DYNC2LI1* c.358C>T mutation in silico prediction shows this missense variant probably damaging. And c.928A>T in exon 12 causes a premature stop codon in 310 of the protein (p.K310X,43), which could lead to truncated protein products or nonsense mediated decay of the mRNA. They were not reported in 1000 Genomes Project, ExAC, HGMD, ClinVar, and other disease databases, and highly conserved from lamprey to human (Figure 3). No mutations in known other skeletal ciliopathy genes or other potential candidate genes were identified. Sanger sequencing was performed to confirm the variants in the family. The pregnant woman carried c.928A>T, and her husband had c.358G>T. It is consistent with an autosomal recessive inheritance model. The same compound heterozygous variants in *DYNC2LI1* were also identified in Fetus 2 (Figure 3). These results provided the definite diagnosis of the affected fetuses: short-rib thoracic dysplasia 15 with polydactyly (SRTD15) (Kessler et al., 2015; Taylor et al., 2015).
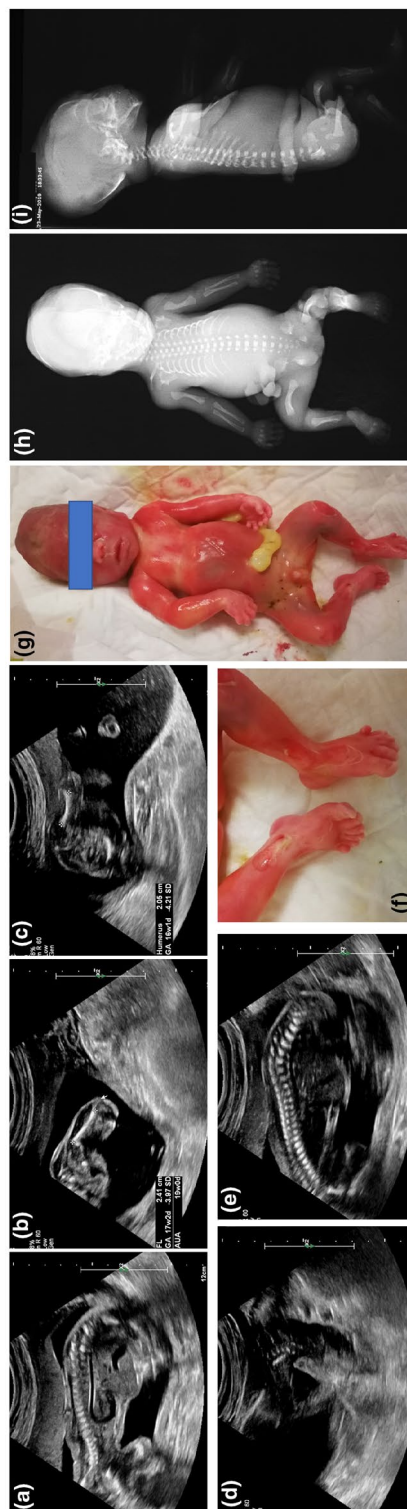

FIGURE 2 (a–e) Prenatal ultrasound of fetus 2 at 21 weeks of gestation. A narrow thorax and an enlarged abdomen (a), shortened limbs (b and c), polydactyly of left foot (d), kyphosis of lumbar vertebra (e). (f and g) Appearance of fetus 2. postaxial polydactyly of feet (f) and appearance of the whole body (g). (h and i) X-ray scaning of Fetus 2 (a markedly narrow thorax and short ribs), frontal X-ray film (h) and lateral X-ray film (i)

TABLE 1 Variations identified in Fetus 1

SNVs/Indels	SNVs	Indels
Initial variants	53,574	6555
Primarily filtering[a]	39,952	3997
Pathogenic, likely pathogenic variants or variants with uncertain significance[b]	1925	1391
Filtering by phenotype and inheritance mode[c]	2	0

[a]Variants in intronic region (beyond 30 bp from exon-intron boundary), SNVs with low-quality (Allele Frequency<0.2, sequencing depth <4x, or mapping qualities <35), InDels in simple sequence repeat region (SSR>7 and Allele Frequency <0.3), and long InDels (length>50 bp) and were preliminarily filtered out.

[b]All the remaining variants were evaluated according to ACMG guideline (Tavtigian et al., 2018). Pathogenic and likely pathogenic variants and variants with uncertain significance were kept.

[c]Variants on genes phenotypically unrelated to the clinical feature of the family were filtered out, and the allele zygosity of variants in accordance with the inheritance mode of the disease were kept. The reference phenotype databases were OMIM (https://www.omim.org/), human phenotype ontology (HPO, https://hpo.jax.org/app/) and Orphanet (https://www.orpha.net/).

4 | DISCUSSION

The defects in genes encoding constitutive and functional protein in cilia could cause ciliopathies (Braun & Hildebrandt, 2017; Zhang et al., 2018). Skeletal ciliopathies featured with narrow thorax and polydactyly were summarized under the term short-rib thoracic dystrophy with or without polydactyly (SRTD), including SRPS, ATD, EVC, and MZSDS (Zhang et al., 2018). The severity in subsets of SRTD differs markedly, spanning from relatively mild to lethal. Now, classification of SRTD is mainly based on underlying genetic causes (Schmidts, 2014). The development of the next generation sequencing (NGS) platform and bioinformatics analysis enables the rapid sequencing of causative genes. 20 pathogenic genes associated with SRTDs are identified so far.

The causative gene of SRTD15 is *DYNC2LI1*, highly expressing in chondrocytes, brain, and kidney in humans (Kessler et al., 2015). *DYNC2LI1* encodes a 351 amino acid light intermediate chain of the dynein-2 complex, which is essential for retrograde intraflagellar transport (IFT) in primary cilia (Asante et al., 2014). Mutations in *DYNC2LI1* can result in the loss of function of DYNC2LI1 to cause shortened and even missing cilia in humans. Taylor et al found that the retrograde IFT defect in *DYNC2LI1* deficient cells led to the accumulation of IFT proteins within the primary cilium (Taylor et al., 2015). Toropova et al. recombinantly expressed the human dynein-2 complex and solved its cryo-EM structure. In the complex, DYNC2LI1 encodes light-intermediate chain (LIC3), which binds both copy of motor-domain-containing heavy chain (DCH2) and stabilizes the structure (Toropova et al., 2019). Compound heterozygosity for

missense, nonsense, and splice site mutations in *DYNC2LI1* could cause SRTD15 (Table 2) (Kessler et al., 2015; Niceta et al., 2018; Taylor et al., 2015). To date, twelve cases in seven families with *DYNC2LI1*-related SRTD15 were described in the literature, and a total of 14 variants of *DYNC2LI1* were identified (Kessler et al., 2015; Niceta et al., 2018; Taylor et al., 2015). Here, we detected two fetuses presenting SRPS-like phenotype by prenatal ultrasound based on remarkably malformed performance in a Chinese family. Owing to phenotypic overlaps among a variety of SRTD, the definite diagnosis was confirmed by genetic testing. The fetuses carried the compound heterozygous variants of *DYNC2LI1*, c.358G>T (p.Pro120Ser; NM_001193464), and c.928A>T (p.Lys310Ter,43; NM_001193464). Both variants were novel. The premature stop codon in 310 of the protein (p.K310X,43) could lead to truncated protein products losing C-terminus, which is very important for the contacts with DCH2, or nonsense mediated decay of the mRNA (Figure 4) (Toropova et al., 2019). We located the reported missense variants and p.Pro120Ser discovery in report to the structure. Interestingly, we found that all the three known missense variants p.Leu117Val, p.Pro120Sser, and p.Thr221Ile located in or near the loops (The dashed frame) connecting alpha helix and beta sheets, indicating that folding of the protein is important for the function of dynein-2 complex (Figure 4).

The reported cases of STRD15 presented with the variability in the severity ranged from prenatal lethality to moderate skeletal dysplasia (Kessler et al., 2015; Niceta et al., 2018; Taylor et al., 2015). Lethality was largely owing to pulmonary hypoplasia secondary to an extremely narrow thorax (Huber & Cormier-Daire, 2012). Those subjects with STRD15 who survived to adulthood didn't suffer from severe cardiorespiratory complications in infancy stage (Niceta et al., 2018). The available prenatal phenotypic features of the affected fetuses showed narrow thorax, postaxial polydactyly, and short limbs, which were often detectable by fetal ultrasound (Table 3). These features of SRTD15 were similar to other SRTDs with mutations in *DYNC2H1*, *TCTEX1D2*, and *WDR34* (Badiner et al., 2017; Gholkar et al., 2015; Huber et al., 2013). Additionally, phenotypic variability among affected individuals with SRTDs was widespread, even in a family (Table 3). Therefore, the overlaps and variability in clinical manifestations in skeletal ciliopathies make it impossible for clinical doctors or genetic counselors to distinguish the subtypes of SRTDs solely based on phenotype. A definitive diagnosis relies on the clinical phenotype in combination with molecular testing. Though the molecular mechanisms underlying these conditions are diverse, combined advances in both genetic investigations and phenotypic collections have been uncovering fetal phenotypes atypical from those classically associated with postnatal conditions of the same genetic disorders (Gray et al., 2019). It is enormously valuable for
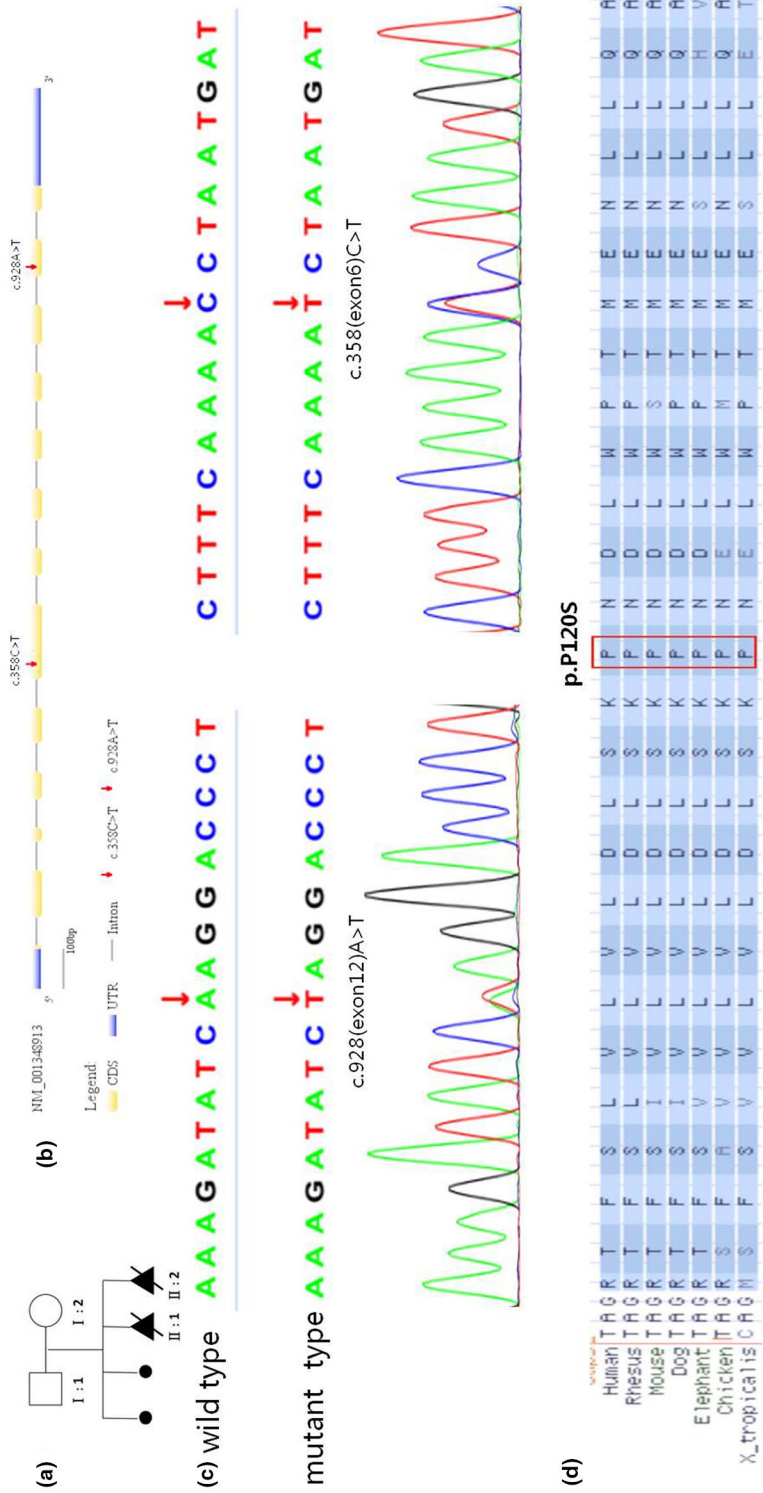
FIGURE 3 Mutations analysis in DYNC2LI1. (a) Pedigree of the family. (b) Genomic structure of DYNC2LI1. Both novel mutations were identified in domain. (c) Sequence chromatogram confirmed that two affected fetuses had the same mutations, and mother and father carried c.928A>T and c.358C>T respectively. (d) Conservation analysis showing that these two mutations in DYNC2LI1 is conserved across human, rhesus, mouse, dog, elephant, chicken and X_tropicalis

TABLE 2 Pathogenic DYNC2LI1 mutations in SRTD15

Subject	Reference	Genomic location (hg19)	cDNA	Exon	Amino acid change	Sift	Polyphen	CADD score v1.3	rs ID/ClinVar	Total MAF (ExAC)	Predicted disruptive effect
Present cases	–	Chr2:44021633	c.358C>T	6	p.Pro120Sser	Deleterious	Damaging	28.7	–	NA	Protein function
		Chr2:44032317	c.928A>T	12	p.Lys310Ter,43	–	–	38.0	rs1336149359	0.0001	Truncating
R01-013A	Taylor et al.	Chr2:44032386	c.996+1G>A	Intron 12	–	–	–	25.0	rs374356079	0.00002	Transcript processing
		Chr2:44021624	c.349C>G	6	p.Leu117Val	Deleterious	Damaging	25.6	rs201948500	0.00003	Protein function
R07-628A	Taylor et al.	Chr2:44021647	c.372G>A	6	p.Trp124Ter	–	–	38.0	rs769975073	0.00004	Truncating
		Chr2:44021624	c.349C>G	6	p.Leu117Val	Deleterious	Damaging	25.6	rs201948500	0.00003	Protein function
R03-303A	Taylor et al.	Chr2:44036850	c.1003G>T	13	p.Glu335Ter	–	–	50.0	rs879255655	NA	Truncating
		Chr2:44032388	c.996+3A>G	Intron 12	–	–	–	13.6	rs879255656	NA	Transcript processing
One family	Kessler et al.	Chr2:44023899	c.622C>T	9	p.Arg208Ter	–	–	45.0	rs745930390	0.00004	Truncating
		Chr2:44027984	c.662C>T	9	p.Thr221Ile	Neutral	Tolerated	23.0	rs886037860	NA	Protein function
Family 1	Niceta et al.	Chr2:44001279	c.2T>C	1	p.Met1?	–	–	20.9	rs200859699	<0.0001	Translation
		Chr2:44027984	c.662C>T	9	p.Thr221Ile	Neutral	Tolerated	23.0	rs886037860	NA	Protein function
Family 2	Niceta et al.	Chr2:44021693	c.420delA	6	p.Val141Ter	–	–	34.0	rs770155116	0.00008	Truncating
		Chr2:44027984	c.662C>T	9	p.Thr221Ile	Neutral	Tolerated	23.0	rs886037860	NA	Protein function
Family 3	Niceta et al.	Chr2: 44004034	c.123_124insA	2	p.Gly42Argfs Ter12	–	–	28.6	–	NA	Truncating
		Chr2: 44027969	c.658-11delT	Intron 8	–	–	–	9.0	rs752971070	0.00001	Transcript processing

Abbreviations: –, absent; +, present; NA, not applicable.
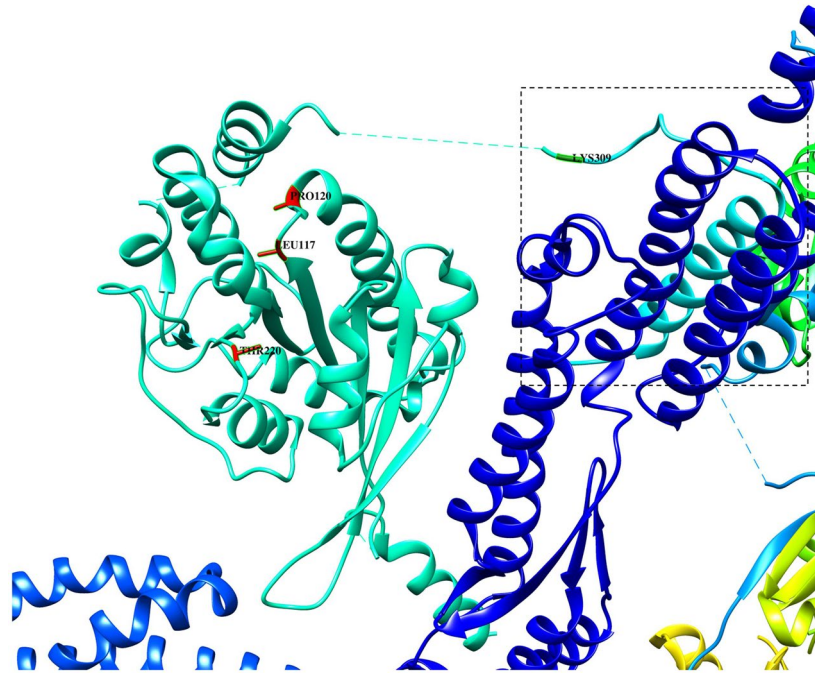
FIGURE 4 The structure of DYNC2LI1 in dynein-2 complex. (a) The known missense variants were located in or near the loops (The dashed frame) connecting alpha helix and beta sheets in the protein; (b) the Cterminus after codon 310 is very important for the contacts of DIC3 with DCH2. p.Thr221Ile and p.Lys310Ter were mapped to codon 220 and 309 in the structure because of different transcripts referred

TABLE 3 Prenatal findings of our cases and four affected fetuses of SRTD15 in the literature

	Our cases		Taylor et al			Kessler et al	
	fetus 1	fetus 2	RO1-013A	R07-628A	R03-303	P3	Total
Fetal sex	M	M	NE	NE	NA	NA	2 M, 4 NA
Weeks of termination of gestation	26 weeks	22 weeks	14 weeks	19 weeks	22 weeks	19 weeks	14–26 weeks
Narrow thorax	+	+	+	+	+	+	6/6 (100%)
Postaxial polydactyly, bands	+	+	+	+	+	+	6/6 (100%)
Postaxial polydactyly, feet	+	+	+	+	+	+	6/6 (100%)
Short limbs	+	+	+	+	+	NE	5/6 (83%)
Kyphosis of lumbar vertebra	+	+	−	−	−	−	2/6 (33%)
Cardiovascular defects	+	−	−	−	−	NE	1/6 (17%)
Transposition of lung and abdominal organs	+	−	−	−	−	NE	1/6 (17%)
Acromphalus	+	−	−	−	−	−	1/6 (17%)
Brachydactyly hands	−	−	+	+	+	NE	3/6 (50%)
Cleft lip	−	−	−	−	−	+	1/6 (17%)

Abbreviations: −, absent; +, present; ETP, elective termination of pregnancy; M, male; NA, not applicable; NE, not evaluable; w, weeks.

genetic counselors to make an accurate molecular diagnosis and manage future pregnancies.

In conclusion, we identified two novel mutations in *DYNC2LI1*, c.358G>T, and c.928A>T, which expanded the spectrum of short-rib thoracic dysplasias with polydactyly types (SRTD)15. WES could enhance the accurate diagnosis in abnormal fetuses, and provide genetic counseling.

CONFLICT OF INTEREST
The authors declare that they have no conflict of interest.

AUTHOR CONTRIBUTIONS

ORCID

Xinyue Zhang https://orcid.org/0000-0002-9336-7586

REFERENCES

Asante, D., Stevenson, N. L., & Stephens, D. J. (2014). Subunit composition of the human cytoplasmic dynein-2 complex. *Journal of Cell Science*, *127*(Pt 21), 4774–4787. https://doi.org/10.1242/jcs.159038

Badiner, N., Taylor, S. P., Forlenza, K., Lachman, R. S., Bamshad, M., Nickerson, D., … Krakow, D. (2017). Mutations in DYNC2H1, the cytoplasmic dynein 2, heavy chain 1 motor protein gene, cause short-rib polydactyly type I. Saldino-Noonan type. *Clinical Genetics*, *92*(2), 158–165. https://doi.org/10.1111/cge.12947

Baker, K., & Beales, P. L. (2009). Making sense of cilia in disease: the human ciliopathies. *American Journal of Medical Genetics. Part C, Seminars in Medical Genetics*, *151c*(4), 281–295. https://doi.org/10.1002/ajmg.c.30231

Braun, D. A., & Hildebrandt, F. (2017). Ciliopathies. *Cold Spring Harbor Perspectives in Biology*, *9*(3), a028191. https://doi.org/10.1101/cshperspect.a028191

Chandler, N., Best, S., Hayward, J., Faravelli, F., Mansour, S., Kivuva, E., … Chitty, L. S. (2018). Rapid prenatal diagnosis using targeted exome sequencing: A cohort study to assess feasibility and potential impact on prenatal counseling and pregnancy management. *Genetics in Medicine*, *20*(11), 1430–1437. https://doi.org/10.1038/gim.2018.30

Elcioglu, N. H., & Hall, C. M. (2002). Diagnostic dilemmas in the short rib-polydactyly syndrome group. *American Journal of Medical Genetics*, *111*(4), 392–400. https://doi.org/10.1002/ajmg.10562

Gholkar, A. A., Senese, S., Lo, Y.-C., Capri, J., Deardorff, W. J., Dharmarajan, H., … Torres, J. Z. (2015). Tctex1d2 associates with short-rib polydactyly syndrome proteins and is required for ciliogenesis. *Cell Cycle*, *14*(7), 1116–1125. https://doi.org/10.4161/15384101.2014.985066

Gray, K. J., Wilkins-Haug, L. E., Herrig, N. J., & Vora, N. L. (2019). Fetal phenotypes emerge as genetic technologies become robust. *Prenatal Diagnosis*, *39*(9), 811–817. https://doi.org/10.1002/pd.5532

Huber, C., & Cormier-Daire, V. (2012). Ciliary disorder of the skeleton. *American Journal of Medical Genetics. Part C, Seminars in Medical Genetics*, *160c*(3), 165–174. https://doi.org/10.1002/ajmg.c.31336

Huber, C., Wu, S., Kim, A. S., Sigaudy, S., Sarukhanov, A., Serre, V., & Cormier-Daire, V. (2013). WDR34 mutations that cause short-rib polydactyly syndrome type III/severe asphyxiating thoracic dysplasia reveal a role for the NF-κB pathway in cilia. *The American Journal of Human Genetics*, *93*(5), 926–931. https://doi.org/10.1016/j.ajhg.2013.10.007

Kearney, H. M., Thorland, E. C., Brown, K. K., Quintero-Rivera, F., & South, S. T. (2011). American College of Medical Genetics standards and guidelines for interpretation and reporting of postnatal constitutional copy number variants. *Genetics in Medicine*, *13*(7), 680–685. https://doi.org/10.1097/GIM.0b013e3182217a3a

Kessler, K., Wunderlich, I., Uebe, S., Falk, N. S., Gießl, A., Helmut Brandstätter, J., … Thiel, C. T. (2015). DYNC2LI1 mutations broaden the clinical spectrum of dynein-2 defects. *Scientific Reports*, *5*, 11649. https://doi.org/10.1038/srep11649

Liu, Y., Wang, L. I., Yang, Y.-K., Liang, Y., Zhang, T.-J., Liang, N. A., & Wu, Q.-Q. (2019). Prenatal diagnosis of fetal skeletal dysplasia using targeted next-generation sequencing: An analysis of 30 cases. *Diagnostic Pathology*, *14*(1), 76. https://doi.org/10.1186/s13000-019-0853-x

Mitchison, H. M., & Valente, E. M. (2017). Motile and non-motile cilia in human pathology: From function to phenotypes. *The Journal of Pathology*, *241*(2), 294–309. https://doi.org/10.1002/path.4843

Mortier, G. R., Cohn, D. H., Cormier-Daire, V., Hall, C., Krakow, D., Mundlos, S., … Warman, M. L. (2019). Nosology and classification of genetic skeletal disorders: 2019 revision. *American Journal of Medical Genetics. Part A*, https://doi.org/10.1002/ajmg.a.61366

Niceta, M., Margiotti, K., Digilio, M. C., Guida, V., Bruselles, A., Pizzi, S., … Tartaglia, M. (2018). Biallelic mutations in DYNC2LI1 are a rare cause of Ellis-van Creveld syndrome. *Clinical Genetics*, *93*(3), 632–639. https://doi.org/10.1111/cge.13128

Petrovski, S., Aggarwal, V., Giordano, J. L., Stosic, M., Wou, K., Bier, L., … Wapner, R. J. (2019). Whole-exome sequencing in the evaluation of fetal structural anomalies: a prospective cohort study. *The Lancet*, *393*(10173), 758–767. https://doi.org/10.1016/s0140-6736(18)32042-7

Schmidts, M. (2014). Clinical genetics and pathobiology of ciliary chondrodysplasias. *Journal of Pediatric Genetics*, *3*(2), 46–94. https://doi.org/10.3233/pge-14089

Simons, A., Shaffer, L. G., & Hastings, R. J. (2013). Cytogenetic nomenclature: Changes in the ISCN 2013 compared to the 2009 edition. *Cytogenetic and Genome Research*, *141*(1), 1–6. https://doi.org/10.1159/000353118

Tavtigian, S. V., Greenblatt, M. S., Harrison, S. M., Nussbaum, R. L., Prabhu, S. A., Boucher, K. M., & Biesecker, L. G. (2018). Modeling the ACMG/AMP variant classification guidelines as a Bayesian classification framework. *Genetics in Medicine*, *20*(9), 1054–1060. https://doi.org/10.1038/gim.2017.210

Taylor, S. P., Dantas, T. J., Duran, I., Wu, S., Lachman, R. S., Nelson, S. F., & Krakow, D. (2015). Mutations in DYNC2LI1 disrupt cilia function and cause short rib polydactyly syndrome. *Nature Communications*, *6*, 7092. https://doi.org/10.1038/ncomms8092

Toropova, K., Zalyte, R., Mukhopadhyay, A. G., Mladenov, M., Carter, A. P., & Roberts, A. J. (2019). Structure of the dynein-2 complex and its assembly with intraflagellar transport trains. *Nature Structural & Molecular Biology*, *26*(9), 823–829. https://doi.org/10.1038/s41594-019-0286-y

Waters, A. M., & Beales, P. L. (2011). Ciliopathies: An expanding disease spectrum. *Pediatric Nephrology*, *26*(7), 1039–1056. https://doi.org/10.1007/s00467-010-1731-7

Zhang, W., Taylor, S. P., Ennis, H. A., Forlenza, K. N., Duran, I., Li, B., … Cohn, D. H. (2018). Expanding the genetic architecture and phenotypic spectrum in the skeletal ciliopathies. *Human Mutation*, *39*(1), 152–166. https://doi.org/10.1002/humu.23362